Soil-Foundation-Structure Interaction with Mobilization of Bearing Capacity: Experimental Study on Sand

V. Drosos[1]; T. Georgarakos[2]; M. Loli[3]; I. Anastasopoulos[4]; O. Zarzouras[5]; and G. Gazetas, M.ASCE[6]

Abstract: Recent studies have highlighted the beneficial role of foundation uplifting and the potential effectiveness of guiding the plastic hinge into the foundation soil by allowing full mobilization of bearing capacity during strong seismic shaking. With the inertia loading transmitted onto the superstructure being limited by the capacity of the foundation, this concept may provide an alternative method of in-ground seismic isolation: the so-called rocking isolation. Attempting to unravel the effectiveness of this alternative design method, this paper experimentally investigates the nonlinear response of a surface foundation on sand and its effect on the seismic performance of an idealized slender single-degree-of-freedom structure. Using a bridge pier as an illustrative prototype, three foundation design alternatives are considered, representing three levels of design conservatism. Their performance is investigated through static (monotonic and slow-cyclic pushover) loading, and reduced-scale shaking table testing. Rocking isolation may provide a valid alternative for the seismic protection of structures, providing encouraging evidence in favor of the innovative idea of moving foundation design toward a less conservative, even unconventional, treatment.
DOI: 10.1061/(ASCE)GT.1943-5606.0000705.

CE Database subject headings: Shallow foundations; Soil-structure interactions; Load bearing capacity; Sand (soil type); Nonlinear response; Bridges; Piers; Shake table tests; Experimentation; Seismic effects.

Author keywords: Shallow foundation; Nonlinear behavior; Bridge pier; Shaking table testing; Experiment; Seismic response; Slow-cyclic pushover.

Introduction

Seismic design of structures recognizes that highly inelastic material response is unavoidable under strong seismic shaking (design earthquake motion). Ductility levels of the order of three or higher are usually allowed to develop at bearing structural elements, and plastic hinging is directed appropriately, therefore the overall stability is maintained (capacity design). By contrast, as reflected in the respective seismic codes, current seismic design practice demands a very conservative treatment of the foundation. Hence, increased factors of safety (FS) and overstrength design ratios are adopted, lest failure be transferred below the ground level. However, this conservative treatment of the foundation, which is designed to retain elastic behavior even for extreme loading, conflicts with modern research findings, indicating that nonlinear foundation response: (1) may be highly probable even for seismic events of moderate intensity, (2) may be favorable for the overall system performance, and (3) may result in permanent deformations that could be restrained within acceptable limits thanks to the transient nature of seismic loading.

[1]Postdoctoral Researcher, National Technical Univ., Athens, Greece.
[2]Doctoral Student, National Technical Univ., Athens 15780, Greece.
[3]Doctoral Student, National Technical Univ., Athens 15780, Greece.
[4]Assistant Professor, National Technical Univ., Athens 15780, Greece.
[5]Graduate Student, National Technical Univ., Athens 15780, Greece.
[6]Professor, National Technical Univ., Athens 15780, Greece (corresponding author). E-mail: gazetas@ath.forthnet.gr

Note. This manuscript was submitted on December 29, 2010; approved on February 6, 2012; published online on February 7, 2012. Discussion period open until April 1, 2013; separate discussions must be submitted for individual papers. This paper is part of the ***Journal of Geotechnical and Geoenvironmental Engineering***, Vol. 138, No. 11, November 1, 2012. ©ASCE, ISSN 1090-0241/2012/11-1369−1386/$25.00.

In the case of shallow foundations, nonlinearity manifests itself through alternating uplift of the foundation (geometric nonlinearity), sliding at the soil-foundation interface (interface inelasticity), and mobilization of bearing-capacity failure mechanisms in the supporting soil (soil inelasticity). When slender structures are considered, rocking motion prevails and the geometric component of nonlinearity dominates.

Earlier studies on rocking structures (Housner 1963; Meek 1978; Priestley et al. 1978; Huckelbridge and Clough 1978; Psycharis and Jennings 1983; Chopra and Yim 1985) have indicated the beneficial role of foundation uplifting on the performance of the supported structure, particularly during severe seismic shaking. Furthermore, allowing for foundation rocking has been proposed by several researchers as an effective method of seismic isolation (Beck and Skinner 1973; Huckelbridge and Ferencz 1981; Priestley et al. 1996; Mergos and Kawashima 2005; Chen et al. 2006; Sakellaraki and Kawashima 2006) and has been applied in the design of modern bridges (e.g., the Rion Antirion Bridge; Pecker 2005). However, in the last decade, the research community has ventured one significant step further, acknowledging that in a way similar to pure uplifting, concurrent inelastic soil response may also help to protect the superstructure against increased seismic demands (Martin and Lam 2000; Pecker and Pender 2000; Faccioli et al. 2001; Gajan et al. 2005; Harden et al. 2006; Pecker 2005; Gazetas et al. 2007; Paolucci et al. 2008; Anastasopoulos et al. 2010a).

The idea of allowing transient mobilization of bearing-capacity failure mechanisms to take place under the foundation level implies the development of an in-soil plastic hinge, whereby the transmitted load is reduced by the limited capacity of the foundation, partially isolating the superstructure from the ground motion. This new foundation design concept suggests that inelastic deformations would accumulate at the soil-foundation system rather than the superstructure elements. Such an analysis

J. Geotech. Geoenviron. Eng. 2012.138:1369-1386.

is nowadays feasible with the availability of a variety of modern numerical tools for modeling the nonlinear rocking behavior and predicting the associated foundation permanent displacements with sufficient accuracy (Allotey and El Naggar 2003, 2008; Cremer et al. 2001, 2002; Chatzigogos et al. 2009; Gajan and Kutter 2008, 2009; Raychowdhury and Hutchinson 2009; Figini 2010; Anastasopoulos et al. 2011).

Under the idealization of rigid base conditions, the rocking motion of a rigid structure supported on shallow foundation is controlled only by its aspect ratio h/L, where h is the height of the center of mass, and L is the foundation breadth (in the direction of loading). Reality is complex because of the nonlinear behavior of the supporting soil. The key parameter controlling the interplay between uplifting and soil yielding during a rocking motion on real (compliant) soil is the ratio of the vertical load N over the ultimate vertical capacity N_{ult}, generally expressed through the safety factor $FS_V = N_{ult}/N$. In addition to being a decisive parameter, FS_V is also easy to determine using traditional bearing-capacity formulae, independently of the characteristics of the seismic excitation.

This paper experimentally investigates the role of nonlinear foundation response on the seismic performance of a slender single-degree-of-freedom structure. The key objectives are the following:

1. Evaluate the effect of soil nonlinearity, uplifting, and mobilization of bearing capacity on the seismic response of the foundation-structure system.
2. Study the role of the two key parameters: the aspect ratio h/L and the vertical factor of safety FS_V.

As schematically illustrated in Fig. 1(a), an idealized bridge pier of moderate height was selected as a typical slender structural system. The pier is founded on dense sand, competent enough to justify the use of a shallow foundation. Keeping the superstructure dead load and the soil properties constant, FS_V and h/L were varied by changing the foundation size. Three different foundations were considered, designated as large, medium, and small, representing a conservatively designed foundation, a less conservative one, and a seriously underdesigned foundation, respectively.

Focusing on foundation rather than superstructure response, the pier is modeled in a simplified manner as a rigid single-degree-of-freedom oscillator, which may translate and rotate as a rigid body. The presented load-displacement data refer to the nomenclature of Fig. 1(b).

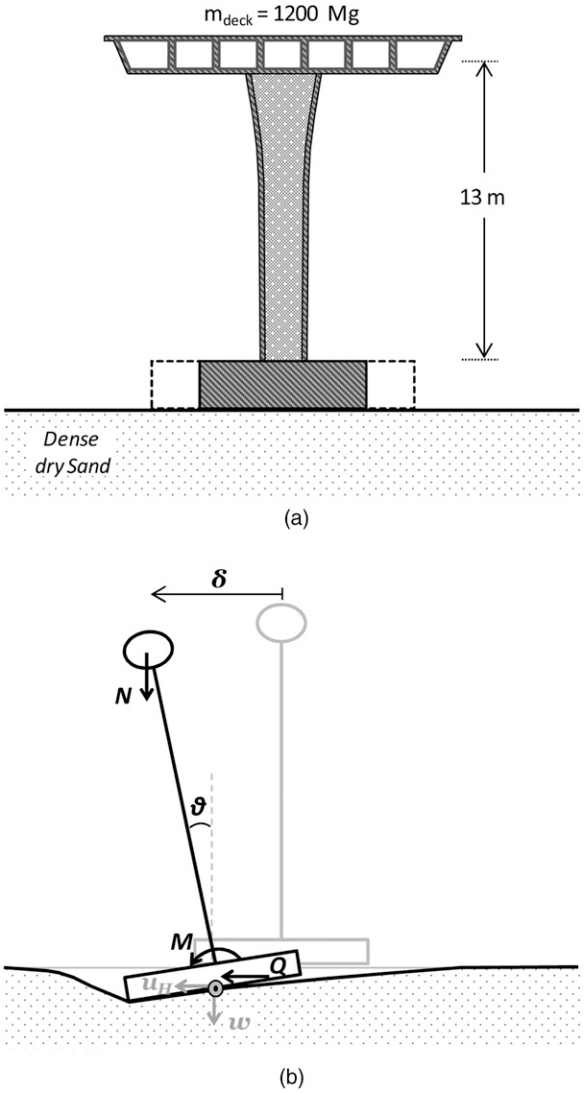

Fig. 1. (a) Problem definition: idealized bridge pier on shallow foundations of varying dimensions; (b) simplified rigid-structure model, showing the notation for loads and displacements

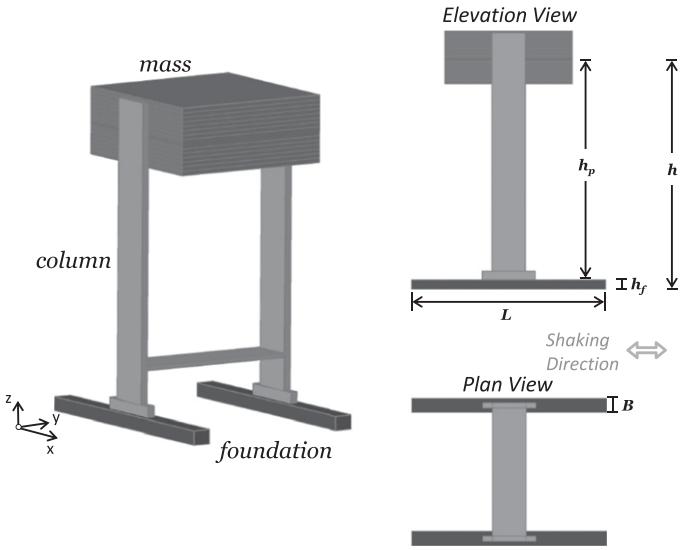

Fig. 2. Geometry of the foundation-structure model

Table 1. Summary of Scaling Laws for 1g Physical Modeling

Quantity	Prototype/model
Length or displacement	N
Area	n^2
Stress	N
Strain	1
Young's modulus	N
Mass	n^3
Density	1
Force	n^3
Moment	n^4
Frequency	$n^{-0.5}$
Acceleration	1

J. Geotech. Geoenviron. Eng. 2012.138:1369-1386.

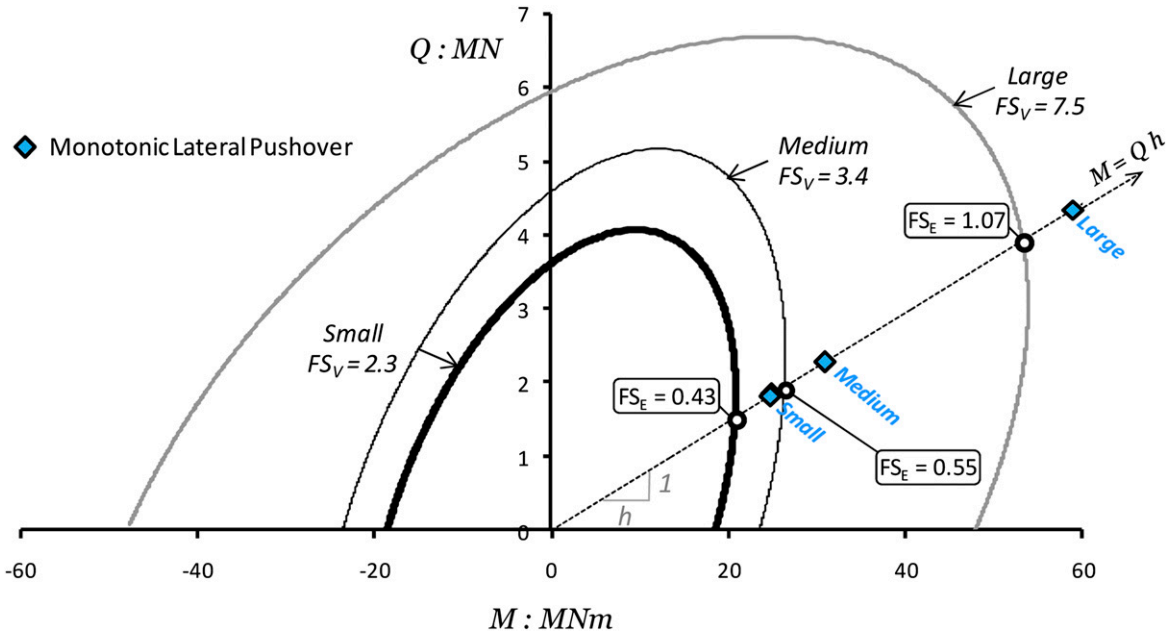

Fig. 3. Prediction of the ultimate horizontal and moment load sustained by the three foundation-structure systems, using the M-Q interaction failure envelopes of Butterfield and Gottardi (1994); the theoretical design values (circles at the intersection of each envelope with the $M = Qh$ line) are compared with the experimental horizontal pushover test results (squares along the $M = Qh$ line)

Methodology

A series of 1g experiments were conducted at the Laboratory of Soil Mechanics of the National Technical University of Athens in order to study the response of the three bridge pier-shallow foundation systems under two conditions: (1) monotonic and slow-cyclic vertical and horizontal (pushover) loading, and (2) seismic shaking. A linear geometric scale of 1/20 ($n = 20$) was selected and model properties (mass, stiffness, excitation period, etc.) were scaled down according to relevant scaling laws (Muir Wood 2004). Unless otherwise stated, the ensuing results are presented in prototype scale.

Soil Sample Preparation and Properties

Dry Longstone sand, an industrially produced fine and uniform quartz sand with $D_{50} = 0.15$ mm and uniformity coefficient $C_u = D_{60}/D_{10} = 1.42$, was used in the experiments. The void ratios at the loosest and densest state have been measured as $e_{max} = 0.995$ and $e_{min} = 0.614$, and the specific weight of the solids was $G_s = 2.64$. The material and strength characteristics of the sand, as derived through a series of laboratory tests, have been documented in Anastasopoulos et al. (2010b).

Nine identical soil specimens were constructed within a rigid container of the dimensions 160 × 90 × 75 cm (at model scale), upon which each one of the pier models was tested separately. The sand was placed into the container through an electronically controlled sand raining system designed to produce soil samples of controllable relative density, D_r, ensuring repeatability.

The initial soil sample was chosen to be of high density, $D_r \approx 85\%$ for all tests, in order to minimize soil densification during shaking. Although reduced-scale testing generally involves low stresses, this is not quite the case here owing to the significant dead load of the structure. Aiming to estimate an effective soil friction angle φ' (i.e., an average friction angle corresponding to the stress level of interest for the particular D_r), a series of vertical pushover tests were performed on three different footing models. Thereby, $\varphi' \approx 44°$ was back-calculated using the classical expressions for ultimate bearing capacity (Meyerhof 1951).

Table 2. Summary of Three Pier-Foundation Systems Geometry and Design Characteristics (in prototype scale)

Property	Large	Medium	Small
Deck mass [M (Mg)]	1,200.00	1,200.00	1,200.00
Pier height [H (m)]	13.60	13.60	13.60
Column height [h_p (m)]	13.00	13.00	13.00
Column section area [A(m^2)]	1.06	1.06	1.06
Column section moment of inertia [I_x (m^4)]	0.32	0.32	0.32
Fixed base period [T_0 (s)]	0.16	0.16	0.16
Foundation length [L (m)]	11.00	7.00	7.00
Width [B (m)]	1.70	1.40	1.14
Slenderness ratio (h/L)	1.20	1.90	1.90
Total vertical load [N (kN)]	14,362.00	13,593.00	13,436.00
Static safety factor (FS$_V$)	7.49	3.41	2.29
Seismic safety factor (FS$_E$)	1.07	0.55	0.43

At this point, the stress field in the supporting soil cannot be correctly reproduced in reduced-scale testing. This is presumed to be the main shortcoming of small-scale testing, which is alleviated by centrifuge model testing. The significantly lower levels of effective stress in the model result in overestimating φ', because the latter is in fact a function of confining stress (Bolton 1986) rather than a constant value, and as a result the soil appears to have larger strength and dilatancy in comparison with the real scale prototype. Nevertheless, 1g shaking table testing is a valid method, provided that such scale effects and the stress-dependent soil behavior are considered in the design of the experiments, and results are interpreted appropriately. Small-scale effects were mitigated, being taken into account in the design of the pier-foundation models, as described in the following section.

J. Geotech. Geoenviron. Eng. 2012.138:1369-1386.

Bridge Pier Modeling in View of Scale Effects

Fig. 2 displays (in three-dimensional, elevation, and plan views) the bridge pier model. The bridge pier is composed of three parts (all made of steel): the mass, column, and elongated foundation. With the exception of the foundation size, the three tested pier models were identical. No attempt was made to model the flexibility and strength of the pier column, and therefore the response is governed solely by the soil-foundation behavior. Owing to the relatively large height of the center of mass (representing the bridge deck), rocking response is expected to prevail, and the behavior is controlled by the two aforementioned parameters: the slenderness ratio of the rigid oscillator, h/L, and the safety factor against bearing-capacity failure for vertical loading, FS_V.

The modeling theory establishes the rules according to which the geometry, material properties, initial conditions, and boundary/loading conditions of the model and the prototype have to be related; therefore, the behavior of the one can be expressed as a function of the behavior of the other, or in other words, the similitude between model and prototype is preserved. Table 1 provides a summary of the scaling laws defining the model-prototype correspondence in single gravity ($1g$) modeling conditions, which have been well established through the use of classical theories of dimensional analysis.

However, when modeling geotechnical problems in reduced scale (i.e., n significantly greater than unity), the similitude is violated by the aforementioned scale effects associated with the stress-dependent soil behavior. Attempting to mitigate this unavoidable shortcoming of $1g$ geotechnical modeling, the three foundation model dimensions were selected appropriately, as to preserve the load-capacity analogy between model and prototype, rather than scaled down geometrically with regard to the scaling laws of Table 1. More specifically, the three foundation model dimensions were back-calculated, in order to instantaneously preserve the load-capacity similarity between model and prototype in both directions of interest (vertical and horizontal in-plane), with regard to preselected prototype ratios of vertical load to vertical bearing capacity (FS_V) and lateral load to lateral capacity ($FS_E = Q/Q_{ult}$ or M/M_{ult}). Recalling that small-scale effects result in overestimation of the soil strength reveals the need to reduce the foundation area disproportionably to what is suggested by the relevant scaling laws, as to satisfy the aforementioned two conditions. Furthermore, given the previously discussed key role of the slenderness ratio h/L in the response of a rocking structure, it is essential that this parameter remains unchanged between model and prototype. Hence, the in-plane foundation dimension L is scaled down from the prototype divided by the scale factor n (hence h/L remains unchanged), whereas the out-of-plane dimension B is further reduced to reduce the foundation area and acquire the desired FS values.

For stability in the out-of plane direction, the deck-mass was supported through a Π shaped column-foundation system, as shown

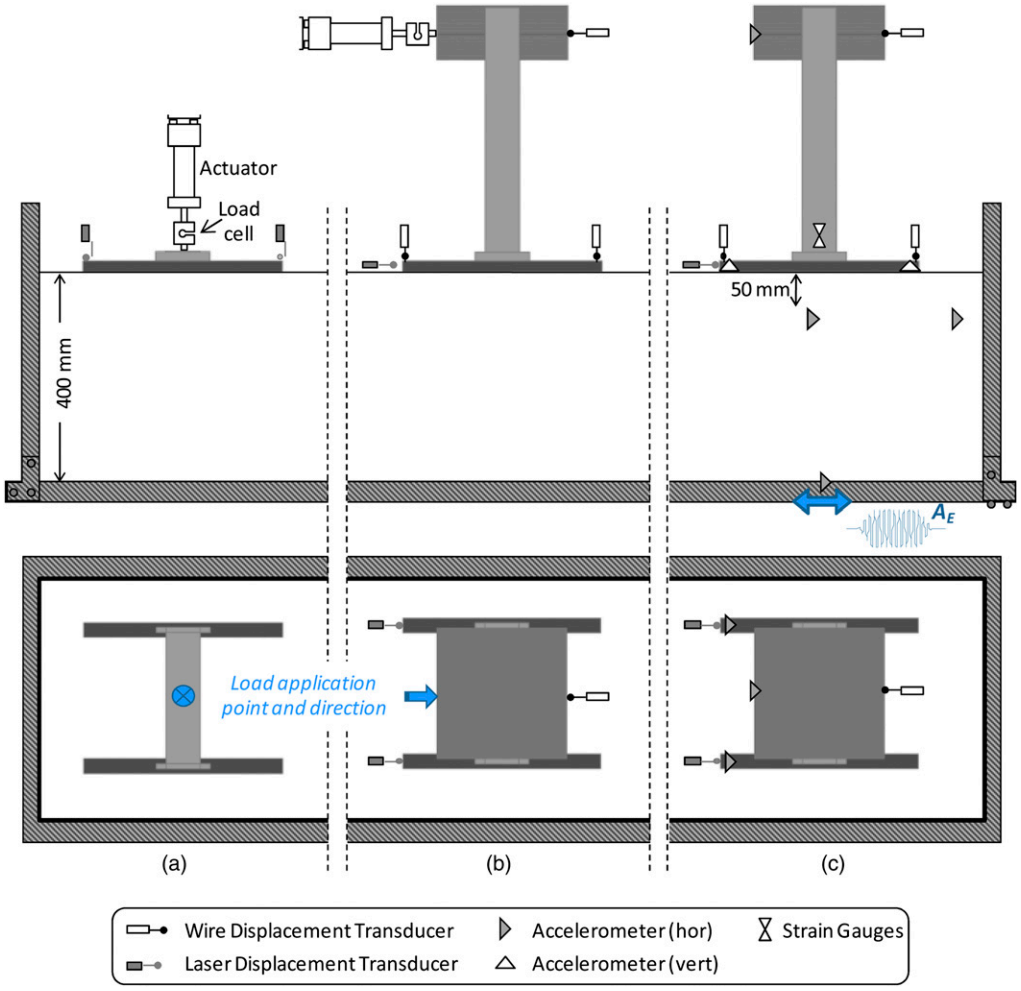

Fig. 4. Experimental set up and instrumentation for (a) vertical pushover; (b) horizontal pushover; (c) shaking table tests

J. Geotech. Geoenviron. Eng. 2012.138:1369-1386.

in Fig. 2, instead of standing upon a single narrow foundation (an idea already utilized in centrifuge model tests at the University of California, Davis by Gajan et al. 2005). Moreover, aiming to produce realistically rough soil-foundation interfaces and provoke a rocking motion to prevail against sliding, sandpaper was placed underneath the foundations, achieving a coefficient of friction of ~0.7.

The utilized foundation models may not be considered as true replica models of the prototype foundations, defined by Moncarz and Krawinkler [1981] as the physical models that totally fulfill similitude requirements, because they ignore foundation shape effects (L/B in the model different than in the prototype). Nevertheless, for the specific problem of nonlinear rocking in one direction, the previously described modeling concept is believed to produce foundation models that adequately reproduce the real (prototype) behavior.

Foundation Design

Bearing-capacity factors have been established in common engineering practice as a simple tool to estimate the ultimate loading of shallow foundations undergoing horizontal (or inclined) and moment (or eccentric) loading (Meyerhof 1953; Vesic 1973). For a variety of reasons (Ukritchon et al. 1998), this traditional approach is currently being replaced by the use of interaction diagrams, that is, envelopes of failure states in the vertical, horizontal, and moment space N-Q-M.

A number of undrained failure envelope analytical formulations can be found in the literature for plane strain and axisymmetric conditions and different interface properties (Bransby and Randolph 1998; Taiebat and Carter 2000; Cremer et al. 2001; Gourvenec 2007). As for foundations resting on sand, the ultimate bearing capacity has been investigated experimentally for strip, rectangular, and circular foundations by Butterfield and Gottardi (1994), Nova and Montrasio (1991), Montrasio and Nova (1997), and Gottardi et al. (1999), respectively.

Based on a large number of experimental results for dense sand (Ticof 1977; Georgiadis and Butterfield 1988; Gottardi and Butterfield 1993), Butterfield and Gottardi (1994) deduced a closed-form expression in the N-Q-M space, which describes the combination of loading that leads to failure

$$\left(\frac{H}{t_h}\right)^2 + \left(\frac{M}{Lt_m}\right)^2 + 2C\frac{MH}{Lt_h t_m} = \left\{\frac{N}{N_u}(N_u - N)\right\}^2 \qquad (1)$$

where t_h, t_m, and C = parameters assumed equal to 0.52, 0.35, and 0.22, respectively (determined through curve fitting of experimental results).

Eq. (1) was utilized for the calculation of transient safety factors against earthquake loading, FS_E, for a design seismic acceleration acting pseudostatically at the center of mass (i.e., the deck). For a constant vertical load N, the ultimate lateral and moment load was determined by the intersection of the M-H failure locus with the load path. The latter is expressed in this simplified problem by the linear relationship $M = Qh$.

Fig. 3 depicts a graphic illustration of the design of the three foundation models for the estimated effective angle of shearing resistance ($\varphi' = 44°$). Although, as previously mentioned, φ' is actually a function of confining stress, a postulation of a constant value is made for the design of all three foundations, mainly because of the very slight variation in the magnitude and distribution of stresses underneath the three of them. This assumption was verified by the back-calculation of φ' from the vertical push test results, which yielded negligible discrepancies from the average value of 44° (φ' ranged from 43.6 to 44.3°).

Despite the considerably larger foundation area (and hence vertical load capacity), the advantage of the medium foundation in comparison with the small is much less pronounced when combined loading is considered. Table 2 summarizes the geometry, elastic properties of column sections, and design characteristics of the three pier-foundation systems. The indicated FS values mark the suitability of each one of the three foundations according to current design requirements. These involve two modes of performance: (1) serviceability under static-permanent loads, which is assured by the demand for $FS_V \geq 2.5$ (or sometimes 3, depending on the bridge type), and (2) resistance to the transient-seismic hazard, which is quantified by FS_E, required to exceed unity for the design seismic action.

Evidently, only the large foundation satisfies both design criteria. The other two unconventionally designed foundations represent two different states of noncompliance with current code requirements. With $FS_V = 3.4$, the medium foundation fulfills code requirements for static loads, but not for seismic with $FS_E = 0.55$, it is expected to respond strongly inelastically under seismic excitation of amplitude equivalent to (or larger than) that of the design motion. Pushing the idea of employing foundation nonlinearity in design to the extreme, the small foundation is underdesigned, although marginally, even for static conditions ($FS_V = 2.3$). For seismic loading, it would be judged as completely inadequate within current design philosophy.

Setup and Instrumentation

The pier model was instrumented to allow direct recording of accelerations, strains, loads, and displacements. Fig. 4 shows the experimental setup and instrumentation for the three test types.

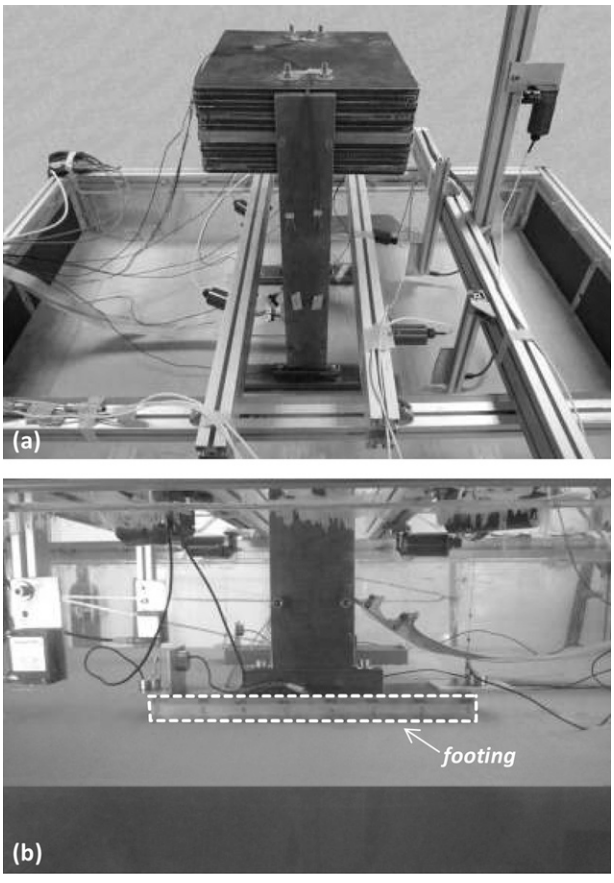

Fig. 5. Photo of the pier model with the small foundation ($FS_V = 2.3$) prior to shaking table testing: (a) three-dimensional view of the model within the strongbox; (b) closer view of the foundation

J. Geotech. Geoenviron. Eng. 2012.138:1369-1386.

During monotonic and slow-cyclic pushover tests, the load was applied in the horizontal or vertical direction through a servoelectric actuator, and measured by a load cell connected at its edge. Wire and laser displacement transducers measured vertical and horizontal displacements of the pier model. In the dynamic (shaking table) tests, the motion of characteristic points within the soil and on the structure were recorded by vertical and horizontal accelerometers, respectively. The strain gauges installed at the base of the column measured section-bending strains. These measurements were used to calculate bending moments at the pier column base, and thereby verify the results derived by the acceleration measurement of the deck-mass. Photos of the small foundation model prior to shaking table testing are shown in Fig. 5.

Pushover Test Results

Before proceeding to the shaking table tests, the response under static monotonic and slow-cyclic pushover loading is discussed. For the sake of brevity, this paper does not include presentation of the results from the vertical push tests, which were conducted to verify the three foundation systems design FS_V values indicated in Table 2.

Lateral Pushover

A suite of lateral pushover tests were conducted, wherein a gradually increasing horizontal displacement was applied at the center of mass of the deck (13.6-m above the foundation level), first monotonically and then slow cyclically. Apart from resembling the cyclic nature of seismic loading and revealing possible differences in system response compared with pure monotonic loading, such cyclic loading also served the purpose of recording the evolution of settlements and the settlement-rotation response of the foundation. Fig. 6 summarizes the moment-rotation (M-θ) and settlement-rotation (w-θ) response of the three foundations, for both types of testing. In the following presentation of results, foundation settlement (w) refers to the additional settlement because of the applied load, which is the output of the total settlement at the specific increment of loading subtracted by the initial static settlement because of the weight of the pier (hence the presented results appear to start from zero settlement). Yet the amount of static settlement was recorded in every test,

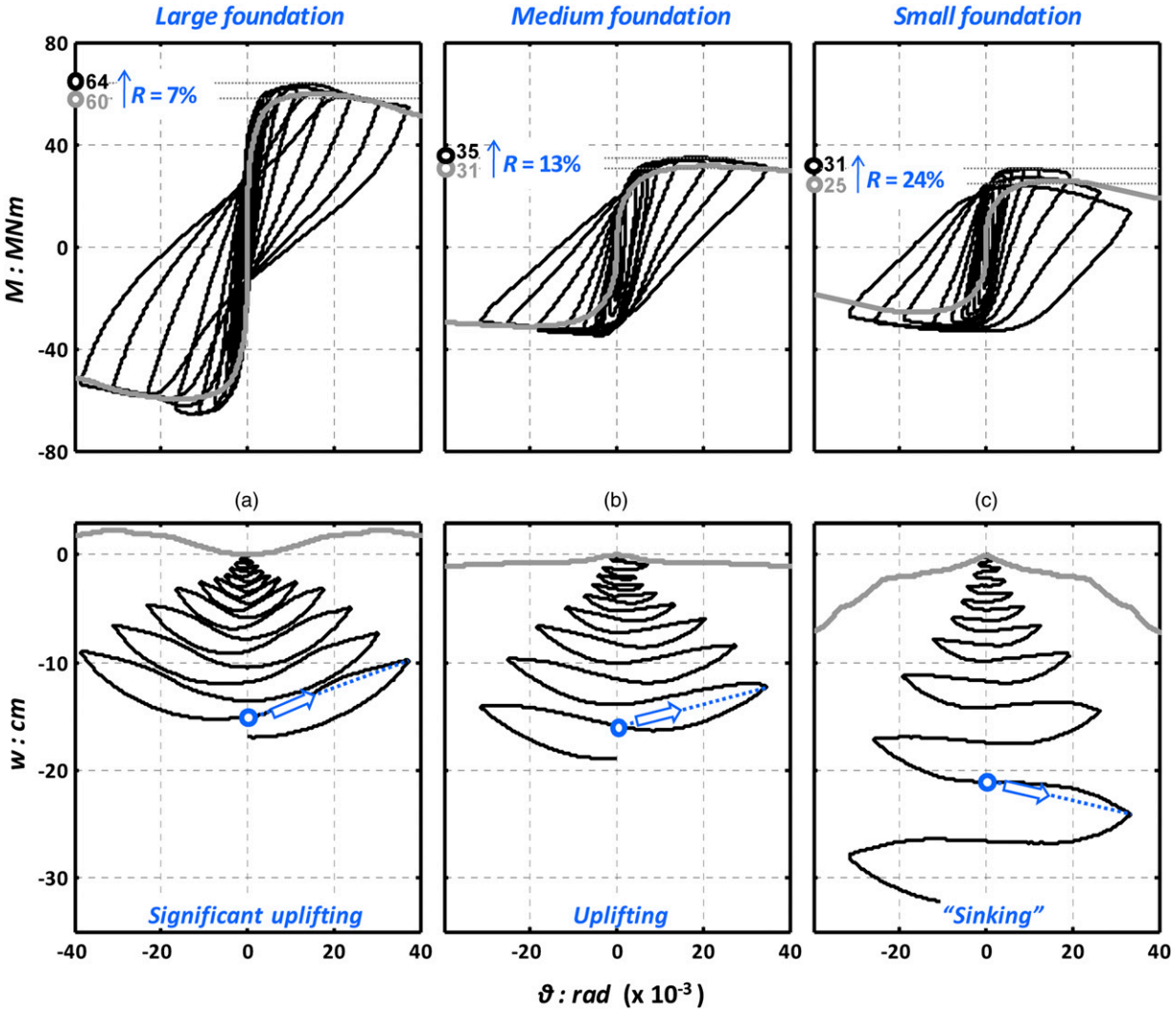

Fig. 6. Monotonic (gray line) and slow-cyclic (black line) lateral pushover test results in terms of moment-rotation and settlement-rotation foundation response: (a) large foundation ($FS_V = 7.3$); (b) medium foundation ($FS_V = 3.5$); (c) small foundation ($FS_V = 2.3$). The settlement refers to the foundation midpoint

J. Geotech. Geoenviron. Eng. 2012.138:1369-1386.

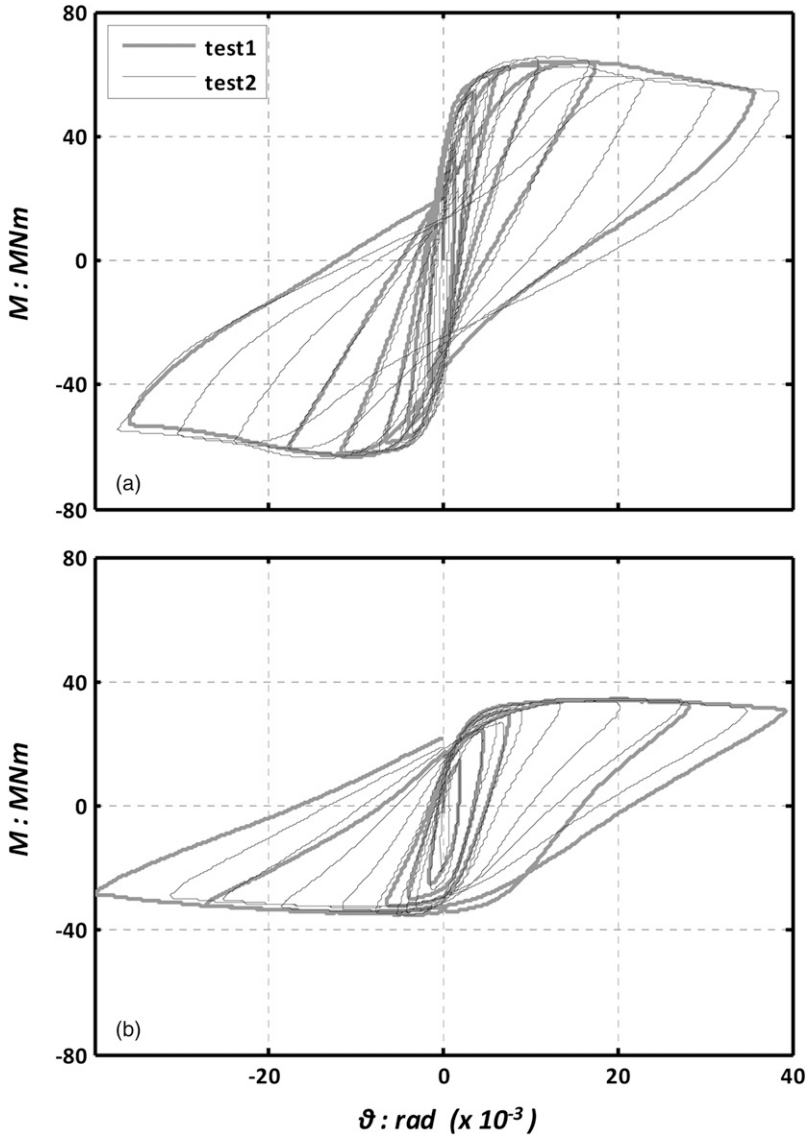

Fig. 7. Verification of repeatability: comparison of two independent lateral pushover tests (Tests 1 and 2) in terms of moment-rotation hysteresis loops: (a) large foundation; (b) medium-size foundation

which was ~3.9 cm for the large foundation pier, 6.1 cm for the medium foundation pier, and 6.9 cm for the small foundation pier (in prototype scale).

Foundation moment capacity primarily depends on foundation size, and hence it comes as no surprise that the large foundation transmits the greatest moment. In particular, when loaded monotonically, it transmits approximately 2 and 2.4 times larger moment than the medium and small foundations, respectively, verifying their design (recall that $FS_E^{large} \approx 2FS_E^{medium} \approx 2.5FS_E^{small}$). However, although the analogy of moment capacity between the three foundations is predicted with excellent accuracy, the comparison is not as satisfactory in terms of absolute values: experimental results exceed somewhat the theoretical-design capacity values. This is clearly illustrated in Fig. 3, through comparison between experimental and theoretical *M-Q* failure points. This underestimation of the actual (measured) lateral foundation capacity (consistently appearing for all three foundations) is presumed to be a result of the postulation of a constant secant friction angle of 44° (determined with reference to vertical pushover test results). The shallower pressure bulbs produced by shear and, especially, moment loading (compared with those produced by vertical loading) would affect soil with larger friction angles, because of smaller vertical stress beyond the footing. Such discrepancies are unavoidable with small-scale modeling.

Switching into cyclic mode appears to have an important effect on the behavior, because it leads to an apparent rotational overstrength. Comparison of cyclic M-θ response with the corresponding monotonic curves (Fig. 6) shows that for the two larger footings the monotonic curves almost envelope the cyclic loops, and with M_{ult} being the same under static and dynamic loading, the cyclic loops of the smaller foundation surpass appreciably the monotonic curve—an apparent cyclic overstrength. Defining the overstrength ratio, R, as the increase in capacity in cyclic loading divided by the capacity under monotonic loading results in the following:

$$R = \frac{\left(M_{\max}{}^{cycl} - M_{\max}{}^{mon}\right)}{M_{\max}{}^{mon}} \tag{2}$$

leads to $R = 24\%$ for the small foundation. Such an apparent overstrength has been observed theoretically for clay and very small FS_V values (<2) by Panagiotidou (2010), and was attributed to the

J. Geotech. Geoenviron. Eng. 2012.138:1369-1386.

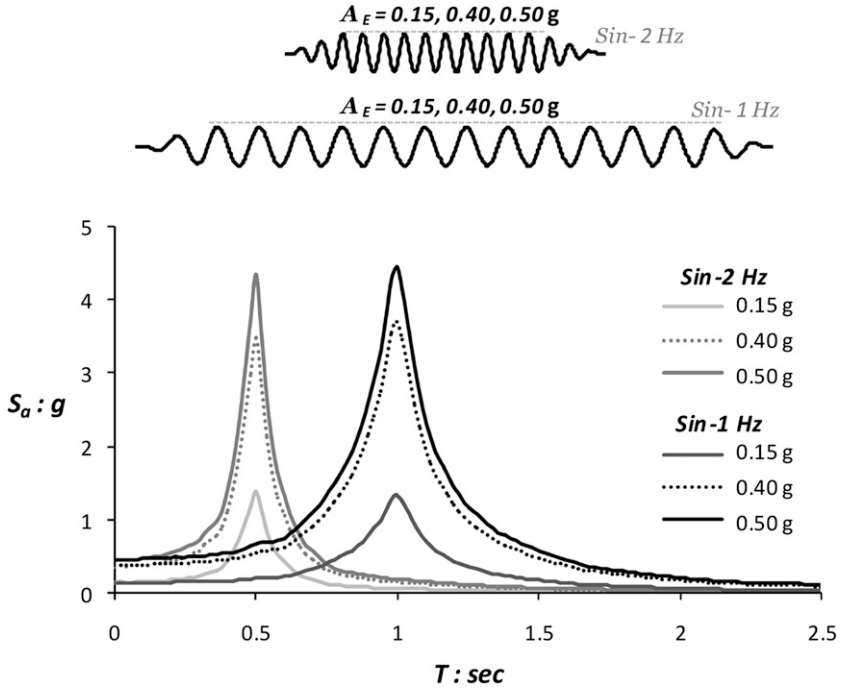

Fig. 8. Acceleration time histories and elastic response spectra of the sinusoidal motions used as (seismic) excitation of the shaking table

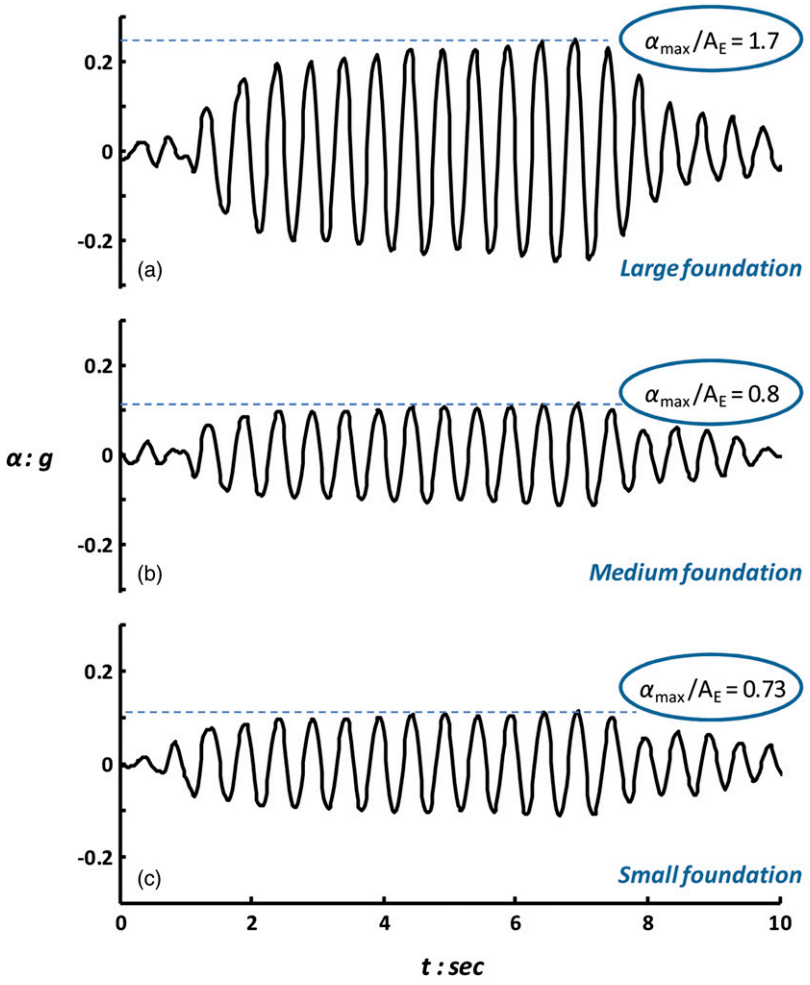

Fig. 9. Acceleration time histories recorded at the level of the deck (center of mass) for base excitation with a 12-cycle 2-Hz sine of 0.15g acceleration amplitude (sin2 − 0.15g) for (a) large foundation ($FS_V = 7.3$); (b) medium foundation ($FS_V = 3.5$); (c) small foundation ($FS_V = 2.3$)

J. Geotech. Geoenviron. Eng. 2012.138:1369-1386.

reversal of the role of P-δ effects when the rotation changes sign. Soil densification, as subsequently explained, may also play an important role. Smaller overstrength values may be observed for the two larger foundations ($R = 13$ and 7% for the medium and large foundations, respectively)—an indication that R increases with increasing FS_V.

The small foundation demonstrates remarkable overstrength, resulting in significantly higher capacity than estimated in design, thus appearing to transmit approximately the same peak moment as the medium-size foundation. These two systems have exactly the same slenderness ratio h/L, which seems to be the most decisive parameter for the ultimate lateral capacity of the rocking systems, perhaps overshadowing the effect of FS_V.

However, despite the lack of a striking effect on moment capacity, FS_V presumably plays a dominant role when foundation displacements are considered. The rocking mode involves uplifting of the foundation at one side and soil yielding at the other, generally resulting in accumulation of (permanent) settlement, as well as (permanent) rotation in the case of asymmetric loading, which is not studied here. This behavior is reflected on the settlement-rotation loops of Fig. 6, where the cyclic movement of the foundation midpoint is depicted as a function of the footing rotation. As expected, settlement increases consistently with reducing FS_V. Hence, although there is only a minor difference among the peak transmitted moments, the small foundation settles almost twice as much as the medium-size foundation.

Furthermore, FS_V controls the interplay between uplifting and bearing-capacity failure mechanisms. The gradient of the settlement-rotation (w-θ) curves indicates whether the foundation midpoint loses contact with the supporting soil as the foundation rotates, giving evidence on the amount of uplift that takes place during the test. Evidently, the large foundation experiences significant uplifting, indicated by the ascending slope of w-θ in Fig. 6(a). Observe that in monotonic loading the large foundation midpoint moves upward almost from the beginning of the loading, revealing that more than half of the foundation detaches from the supporting soil.

As FS_V reduces, soil nonlinearity (i.e., mobilization of the bearing-capacity failure mechanism) becomes prevalent, resulting in greater rates of settlement per cycle, and reducing the extent of foundation uplift. Monotonic w-θ curves [Figs. 6(b and c)] clearly show downward movement of the foundation midpoint with rotation, for both the medium-size and the small foundation. Yet, the significant difference in their inclination indicates some limited uplifting of the medium-size foundation in contrast to the sinking response of the small foundation. Interestingly, the w-θ gradient of the medium-size foundation reverses after a few cycles of loading, showing upward movement of the foundation midpoint and hence reduction of the minimum soil-foundation contact area, possibly as a result of sand densification (i.e., compaction) under the oscillating footing.

This is not the case for the small foundation. The increased structural weight relative to the foundation capacity makes uplifting much more energy-consuming than soil yielding, which thus takes place for smaller foundation rotation. The supporting soil complies

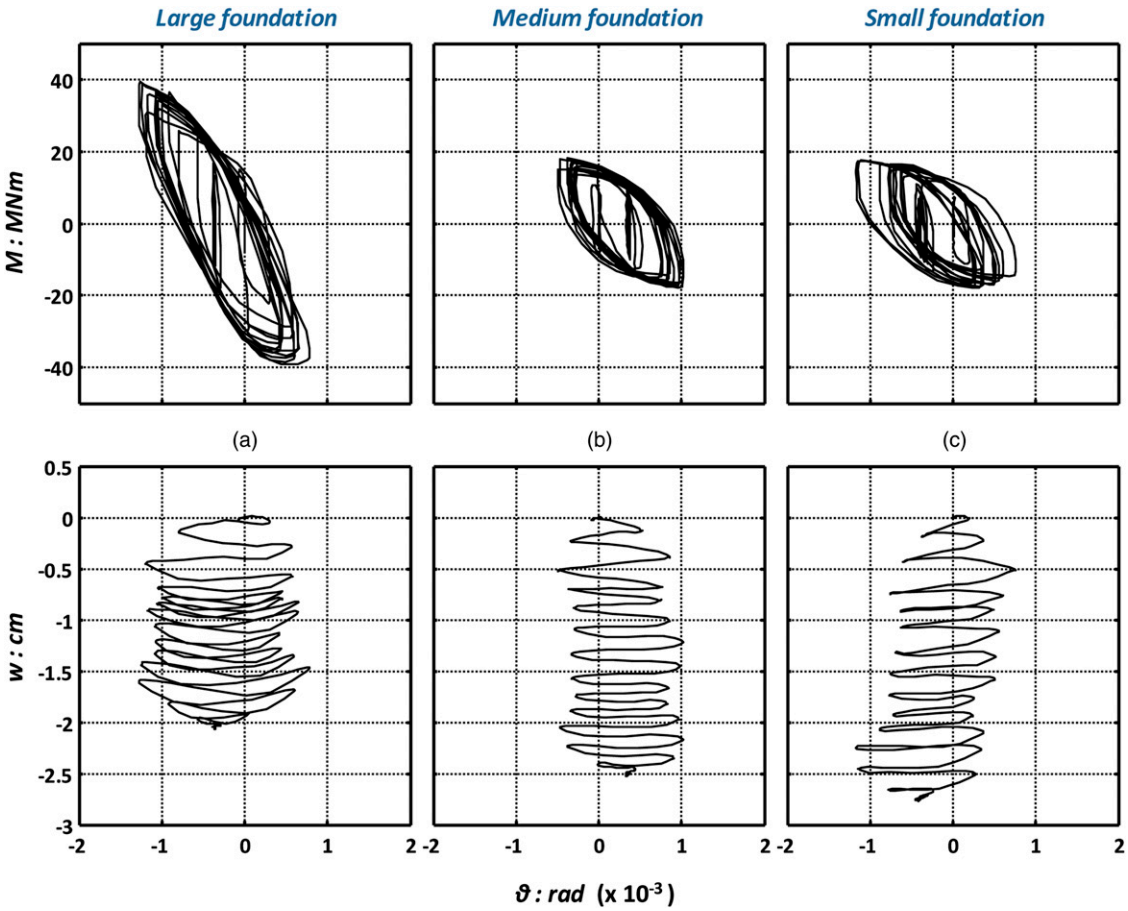

Fig. 10. Foundation response to base excitation of a 12-cycle 2-Hz sine with $0.15g$ acceleration amplitude ($\sin 2 - 0.15g$); evolution of moment-rotation and settlement-rotation hysteretic response for (a) large foundation ($FS_V = 7.3$); (b) medium foundation ($FS_V = 3.5$); (c) small foundation ($FS_V = 2.3$)

J. Geotech. Geoenviron. Eng. 2012.138:1369-1386.

as the foundation rotates, and the foundation midpoint settles in every half-cycle of loading, increasing dramatically the amount of settlement per cycle. In fact, this rapid accumulation of settlement during cyclic loading is believed to be a second reason for the observed foundation overstrength, explaining why the phenomenon becomes more significant for low FS_V values.

Aiming to ensure the validity and repeatability of the testing procedure and gain confidence in the presented data, the lateral pushover test for the large and the medium foundation were repeated and, indeed, gave quite similar results. As an example, the comparison of M-θ loops (Fig. 7) shows quite satisfactory agreement between the results of original and repeat tests (Test 1 and 2). Tests 1 and 2 involved quite different displacement loading histories in terms of sequence and number of cycles; therefore, the produced response loops reasonably indicate different foundation rotation histories. Yet, their comparison is excellent in terms of ultimate moment capacity and stiffness degradation with increasing rotation (observe the very similar inclination of the curves for similar amplitudes of rotation).

Furthermore, the results of Figs. 6 and 7 are in excellent qualitative accord with the experimental results obtained in the large-scale sand box of the European Laboratory for Structural Assessment documented by Negro et al. (2000), and in the centrifuge tests at the University of California, Davis (Gajan et al. 2005).

Shaking Table Test Results

The three soil-foundation-pier systems were then subjected to shake table testing, using a variety of seismic motions (artificial and real records) as the base excitation. Because of space restrictions, this paper focuses on symmetric harmonic excitations (i.e., sinusoidal motions), while the effect of excitation asymmetry and directivity effects (i.e., real records) will be discussed in a subsequent publication.

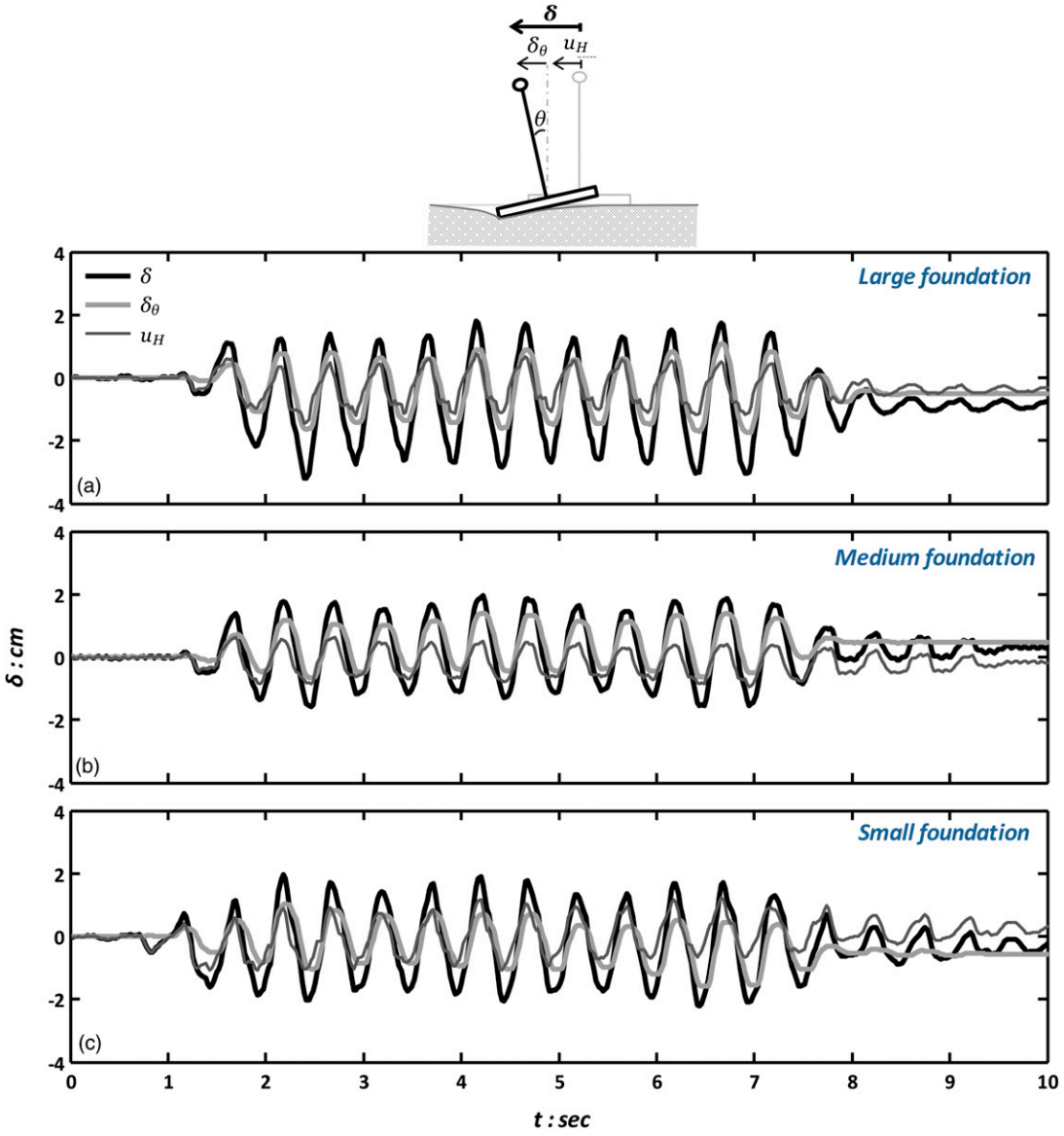

Fig. 11. Time histories of deck displacement δ, decoupled into its rotational $\delta_\theta = \theta h$ and swaying u_H components for base excitation with a 12-cycle 2-Hz sine of $0.15g$ acceleration amplitude ($\sin 2 - 0.15g$) for (a) large foundation ($FS_V = 7.3$); (b) medium foundation ($FS_V = 3.5$); (c) small foundation ($FS_V = 2.3$)

J. Geotech. Geoenviron. Eng. 2012.138:1369-1386.

Each of the three systems was subjected to six successive seismic events, wherein a 12-cycle sine pulse of varying acceleration amplitude was input at the model base (representing bedrock). The sequence of the seismic motions was selected in such way to study the effect of two parameters: (1) the maximum acceleration amplitude, A_E, and (2) the excitation frequency, f_E. First, the model was subjected to three sine motions of $f_E = 2$ Hz, gradually increasing A_E (0.15, 0.4, and $0.5g$). Then, the same excitation sequence, with respect to A_E, was repeated for $f_E = 1$ Hz. Fig. 8 shows the acceleration elastic response spectra (for damping $\xi = 5\%$) of the six bedrock sine excitations.

In the framework of elasticity, the response of an oscillator to such harmonic dynamic excitation is determined by the relationship between the excitation frequency, f_E, and its natural frequency, f_0, while being proportional to the excitation intensity. Under nonlinear conditions, however, two counteracting mechanisms take place. First, the natural period of the system is an increasing function of deformation amplitude, and hence of the excitation intensity (i.e., of A_E); second, and possibly most importantly, the limited capacity of the foundation sets a well-defined limit on the magnitude of inertial forces that can develop in the mass of the oscillator.

More specifically, the maximum (critical) acceleration, α_c, that can be transmitted to the mass of the rocking pier-foundation system is directly related (by Newton's law) to the moment capacity of the foundation, M_{ult}, by the following relationship: $\alpha_c = M_{ult}/mgh$. Hence, with reference to the ultimate moment capacity determined by pushover tests, the large foundation system may sustain $\alpha_c \approx 0.37g$. Having about half the moment capacity of the large foundation, the two smaller foundations should cut off the seismic motion transmitted to the superstructure to a much lower level: $\alpha_c \approx 0.19$ and $0.16g$, for the medium and the small foundation, respectively. This rocking isolation mechanism, presumably associated with full mobilization of foundation-soil moment capacity (expressed as uplifting and soil yielding), forms the cornerstone of the new idea for allowing, and taking advantage of, nonlinear foundation response. This is illuminated in the sequel through the shaking table results.

Moderate Intensity Seismic Excitation

A sinusoidal motion of $f_E = 2$ Hz and $A_E = 0.15$ g is studied first, as an example of a moderate-intensity seismic excitation. The dynamic response of the three systems is depicted in Fig. 9 in terms of acceleration time histories recorded at the deck level (i.e., at the oscillator mass). The conservatively designed pier (large foundation) experiences two times more intense shaking than the other two (medium and small foundation), amplifying the input seismic acceleration by a factor of $\alpha_{max}/A_E \approx 1.7$. By contrast, with the two smaller foundations, the seismic motion is

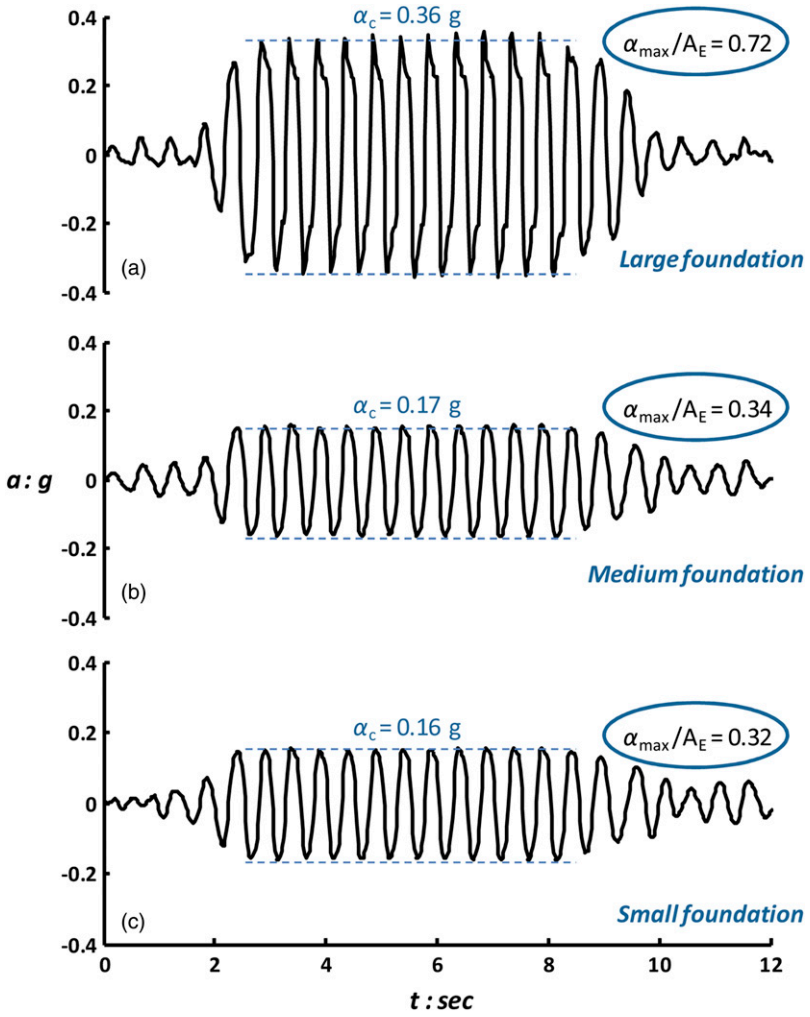

Fig. 12. Acceleration time histories recorded at the level of the deck for base excitation of a 12-cycle 2-Hz sine with $0.50g$ acceleration amplitude (sin2 − $0.50g$) for (a) large foundation ($FS_V = 7.3$); (b) medium foundation ($FS_V = 3.5$); (c) small foundation ($FS_V = 2.3$)

J. Geotech. Geoenviron. Eng. 2012.138:1369-1386.

reduced to $\alpha_{max}/A_E = 0.8$ and 0.73 for the medium and the small foundation, respectively.

Observe that the deck acceleration amplitude is, in all three cases, below the critical values previously estimated, which suggests that, at this level of seismic intensity, the response is not affected by the ultimate capacity of the foundation and the related rocking isolation mechanism. The moment-rotation loops in Fig. 10 vindicate this argument, showing that the three foundations respond in the nonlinear range but well below their ultimate capacity. The evident hysteretic behavior is attributed to the nonlinearity of the supporting soil, which precedes the development of failure mechanisms.

Hence, the observed amplification in the case of the large foundation, and the corresponding attenuation for the two smaller ones, is mainly the result of the frequency dependency of the oscillatory response. In other words, the stiffer large foundation system presumably vibrates within an effective dominant period range close enough to that of the input excitation ($f_E = 2$ Hz), resulting in dynamic amplification of the input motion. In contrast, the effective period of the two smaller foundation oscillators is substantially larger (owing to intensely nonlinear response), resulting in dynamic attenuation of the input motion. Consequently, but rather unexpectedly, despite having about a two times larger factor of safety against seismic loading (FS_E), owing to such tuning/detuning phenomena, the large foundation experiences larger rotation compared with the underdesigned foundation systems and only a slightly smaller (permanent) settlement (2 cm, compared with 2.5 and 2.8 cm) than the other two (Fig. 10).

An equally effective way to assess the performance of the three pier-foundation system is through lateral deck displacement. In the particular case of a practically rigid pier, the total horizontal displacement at the deck level would be a result of two components: the horizontal translation-swaying displacement of the system, u_H, and the additional displacement, δ_θ, because of foundation rotation. Fig. 11 presents the drift response of the deck in the time domain, showing the contribution of these two components. Despite the rocking susceptibility of the studied systems, the input motion in this case is relatively low to cause significant foundation uplifting or yielding, if at all, which results in the rotational component of deck displacement being comparable with its horizontal translation.

Again, the comparison favors the piers standing on the medium and small foundations, while the conservatively designed system experiences deck displacement of significantly larger amplitude. Nevertheless, at this excitation level, the displacement values are in every case relatively small, and would be easily accommodated by the bridge superstructure.

Severe Seismic Excitation

Increasing the acceleration amplitude of the input motion to $A_E = 0.5g$ for the same dominant frequency ($f_E = 2$ Hz) results in the

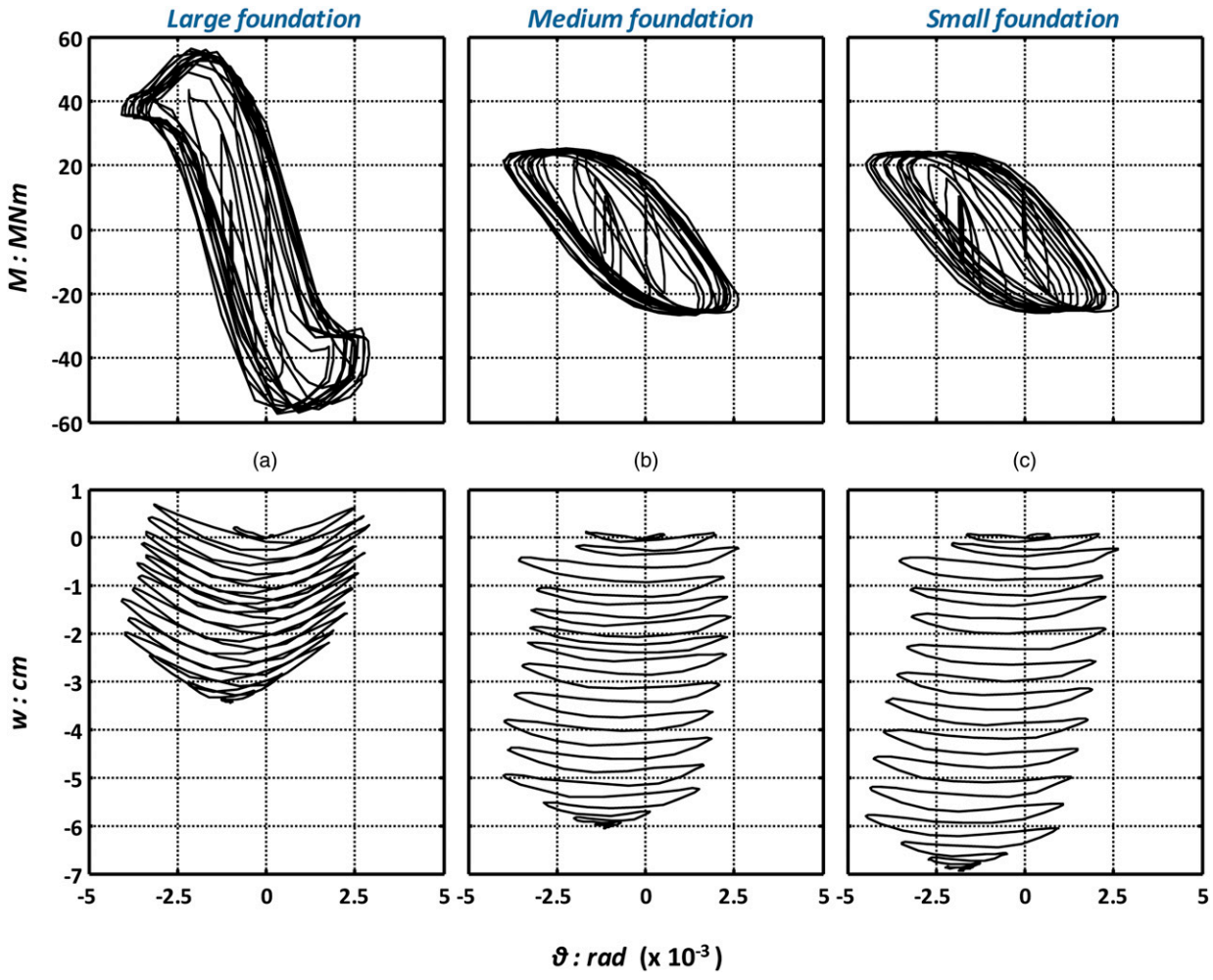

Fig. 13. Foundation response to base excitation of a 12-cycle 2-Hz sine pulse with $0.50g$ acceleration amplitude ($\sin 2 - 0.50g$); moment-rotation and settlement-rotation response for (a) large foundation ($FS_v = 7.3$); (b) medium foundation ($FS_v = 3.5$); (c) small foundation ($FS_v = 2.3$)

J. Geotech. Geoenviron. Eng. 2012.138:1369-1386.

response being highly nonlinear for all three foundations, with the rocking isolation mechanism playing a dominant role. The acceleration time histories of the deck (Fig. 12) are strictly cut off at a particular critical value for each one of the three systems. The latter are in remarkable agreement with the previously discussed rough estimates on the basis of static tests α_c values. The two underdesigned foundation systems provide a more drastic reduction of the seismic acceleration transmitted to the pier to only one-third of the input peak acceleration. Some limited isolation effects are observed, even in the case of the large foundation system ($\alpha_{\max}/A_E = 0.72$). Yet, having a significantly larger capacity M_{ult} compared with the other two systems, the conservatively designed pier suffers much more intense shaking.

Fig. 13 depicts the moment-rotation and settlement-rotation loops of the three systems. Once again, the large foundation experiences the rotational motion of similar or larger amplitude than the two smaller foundations, because its advantage of having larger moment resistance and rocking stiffness is counterbalanced by the two times greater inertial loading that it suffers. The large foundation pier appears to experience appreciably larger deck drift, which is primarily a result of foundation rotation for this high excitation level (Fig. 14). Hence, as for the previous case ($A_E = 0.15g$), the only benefit of design conservatism is the reduction of foundation settlement to one-half the value of the most daring systems. As expected, compared with the previously discussed smaller magnitude base excitation, the settlements of all three systems are now

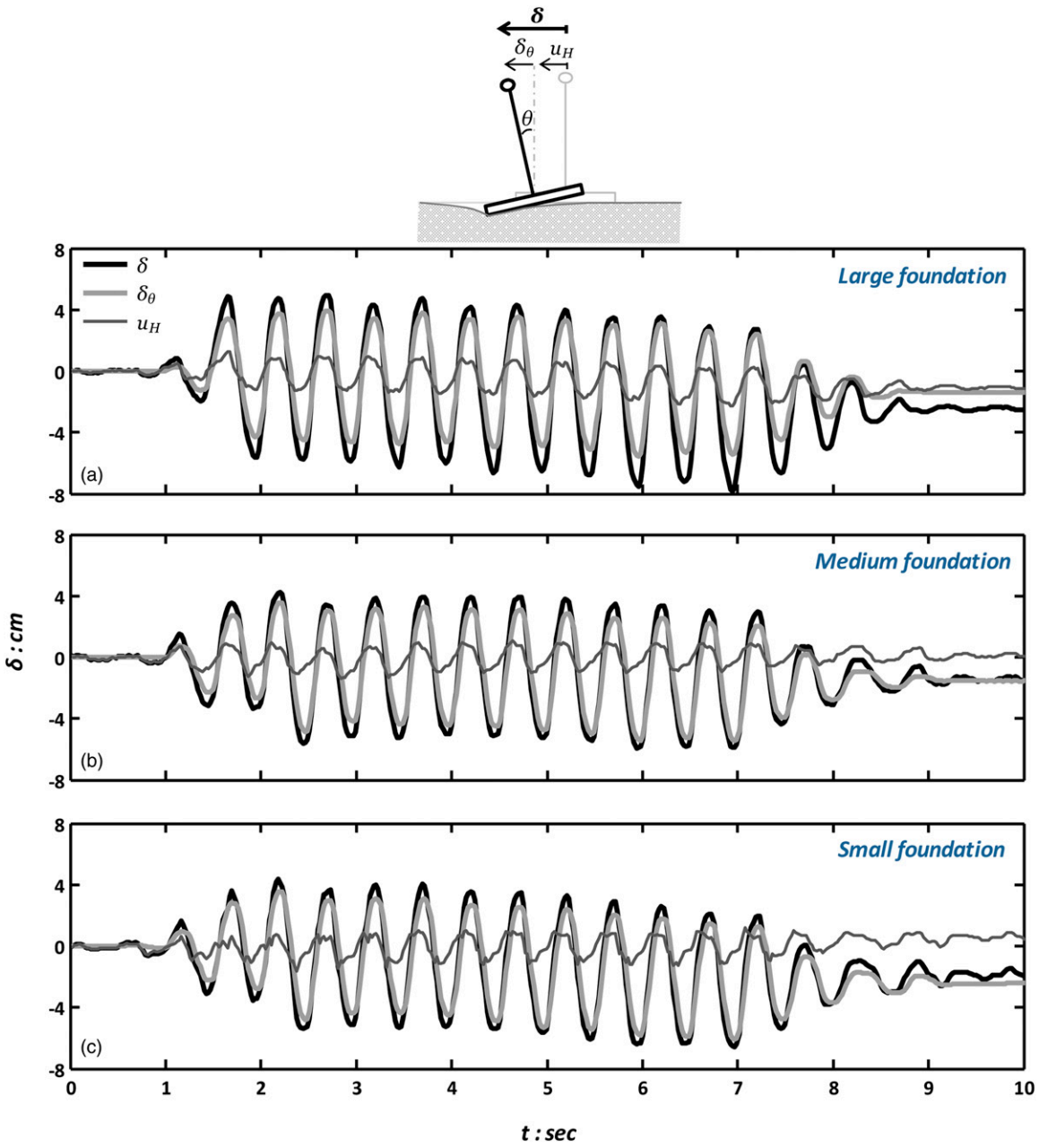

Fig. 14. Time histories of deck displacement δ, decoupled into its rotational $\delta_\theta = \theta h$ and swaying u_H components for base excitation with a 12-cycle 2-Hz sine pulse of $0.50g$ acceleration amplitude ($\sin 2 - 0.50g$) for (a) large foundation ($FS_V = 7.3$); (b) medium foundation ($FS_V = 3.5$); (c) small foundation ($FS_V = 2.3$)

J. Geotech. Geoenviron. Eng. 2012.138:1369-1386.

significantly larger, reaching a maximum of 3.5 cm for the large and 7 cm for the small foundation.

Effect of Seismic Excitation Frequency

To study the effect of excitation frequency, f_E, the three systems are subjected to a sine excitation of the same acceleration amplitude, but of frequency $f_E = 1$ Hz. The reduction of f_E has a drastic effect on system response, as demonstrated by foundation moment-rotation and settlement-rotation curves (Fig. 15), and the deck displacement time histories (Fig. 16). Observe the apparent gradual degradation of the moment-rotation stiffness in all three cases, which results in a rotational motion 3 times larger than with the $f_E = 2$ Hz seismic excitation (10×10^{-3} rad instead of roughly 3×10^{-3} rad). Even the small foundation exhibits sizable uplifting behavior (evident by the ascending gradient of the settlement-rotation curves in Fig. 15), while the large one demonstrates a spectacular 5 cm lift-off of its middle point. This uplifting-dominated behavior of the small foundation is believed to be the result of soil densification occurring during the preceding seismic excitation cycles (note that sin1 $-0.5g$ was the last excitation of the testing sequence).

Despite the mentioned differences, the previously discussed conclusions regarding the effect of foundation size on the inertial forces and the resulting system displacements (deck drift and foundation settlement) remain valid for this excitation. The only difference refers to an increase in foundation capacity (overstrength) mainly because of the settlement acquired during the preceding excitations.

Conclusions

An experimental study with carefully controlled testing conditions has been presented, aiming primarily at investigating the effect of shallow-foundation nonlinear behavior on the response of structure-foundation systems. To focus on the rocking mode of foundation response, a 13-m tall bridge pier was modeled, representing a typical, rocking susceptible slender structure. Three foundation alternatives were investigated, designated as large, medium, and small, representing three levels of design conservatism (Table 2). Results are shown for static (monotonic and slow-cyclic) loading, as well as for seismic shaking with 12-cycle sine pulses of varying magnitude and frequency. The main conclusions can be summarized as follows:

1. A significant outcome is the experimental verification—proof of concept—of the potential effectiveness of rocking isolation as a means of seismic protection of a bridge pier. Encouraging evidence has been provided in favor of the idea of changing the philosophy of foundation design toward a less conservative, even unconventional, treatment. Acting as a safety fuse, full mobilization of foundation capacity (in the form of uplifting and soil yielding) constrains the acceleration transmitted onto

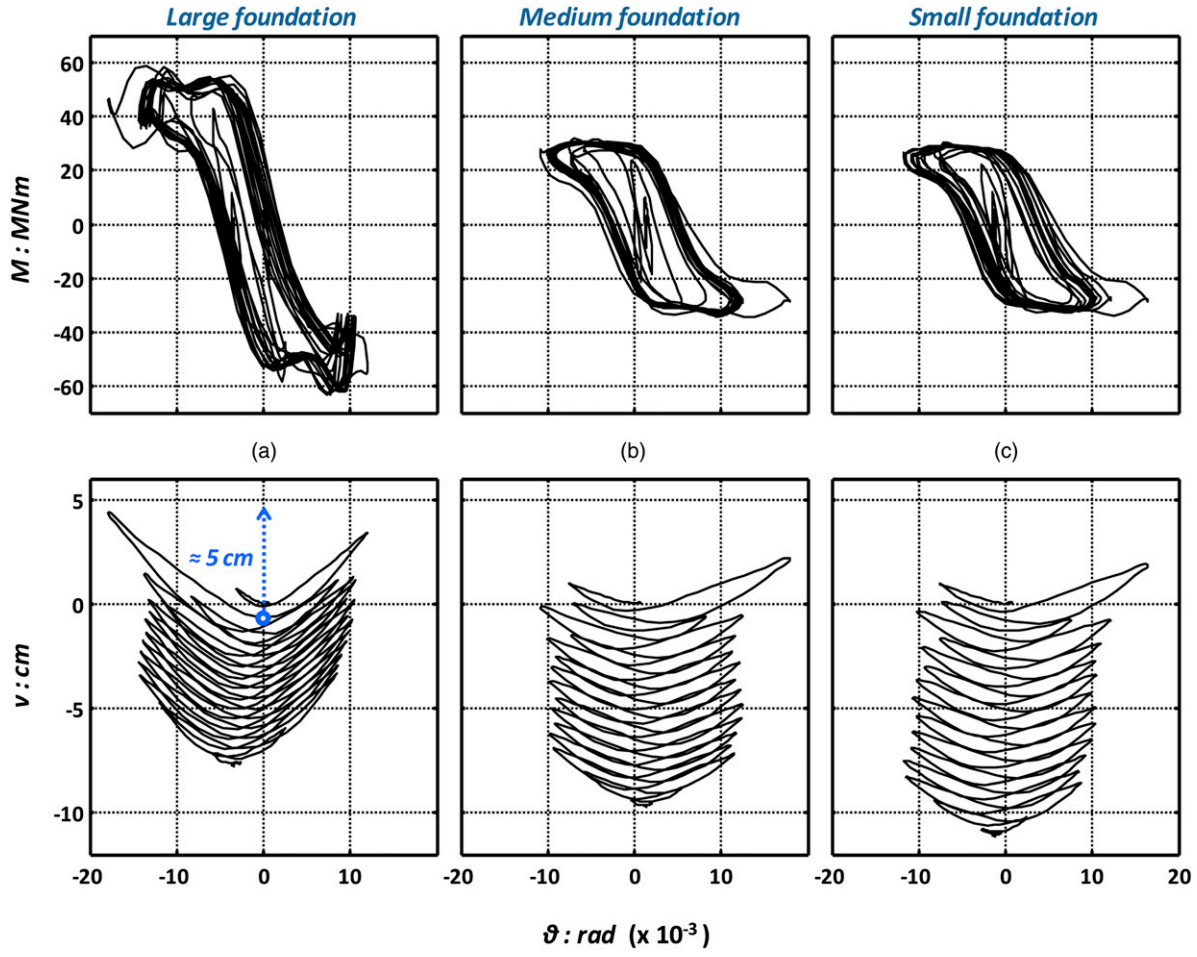

Fig. 15. Foundation response to base excitation of a 12-cycle 1-Hz sine with $0.50g$ acceleration amplitude (sin1 $- 0.50g$); evolution of moment-rotation and settlement-rotation hysteretic response for (a) large foundation ($FS_V = 7.3$); (b) medium foundation ($FS_V = 3.5$); (c) small foundation ($FS_V = 2.3$)

J. Geotech. Geoenviron. Eng. 2012.138:1369-1386.

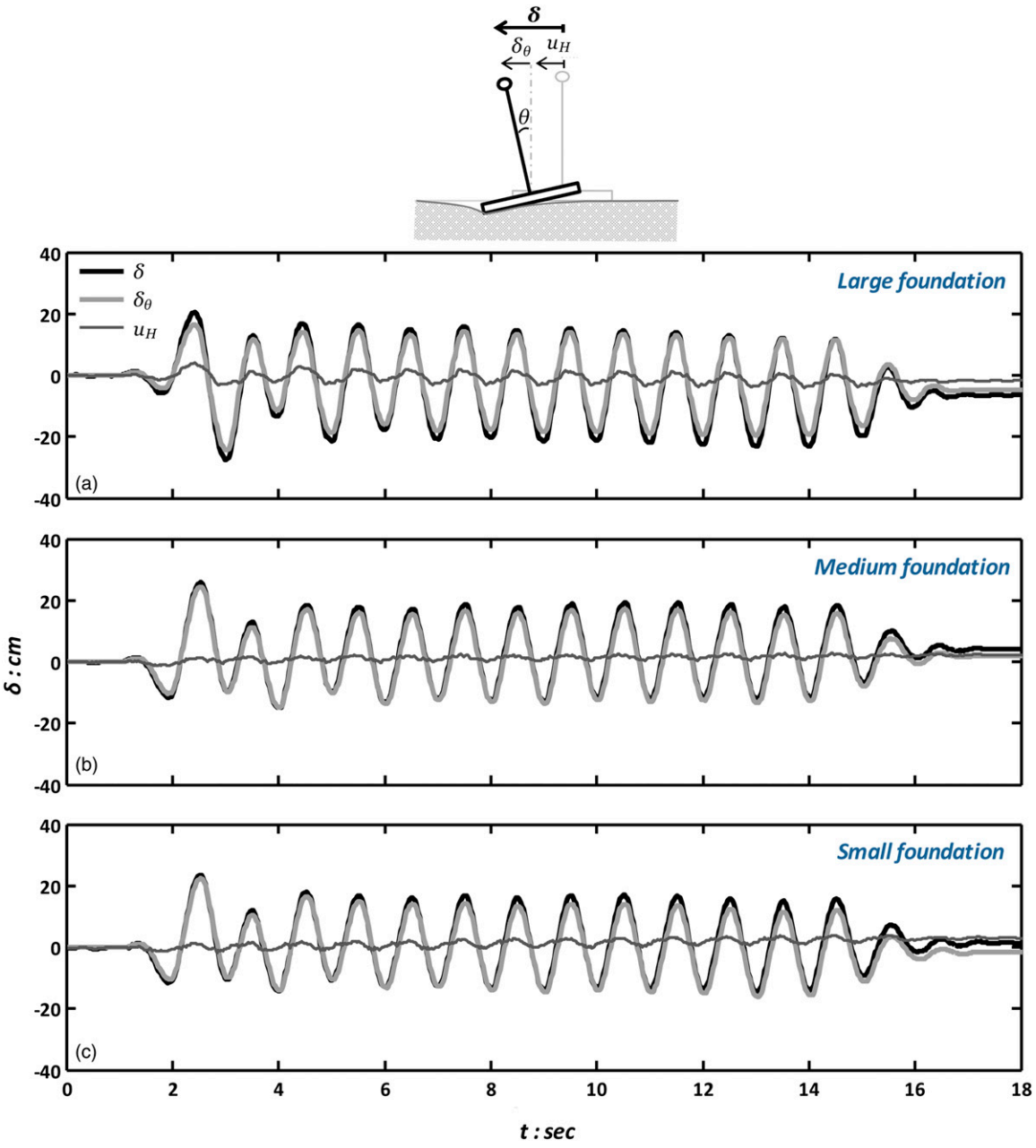

Fig. 16. Time histories of deck displacement δ, decoupled into its rotational $\delta_\theta = \theta h$ and swaying u_H components for base excitation with a 12-cycle 1-Hz sine pulse of $0.50g$ acceleration amplitude ($\sin 1 - 0.50g$) for (a) large foundation ($FS_V = 7.3$); (b) medium foundation ($FS_V = 3.5$); (c) small foundation ($FS_V = 2.3$)

the superstructure to a value below a critical acceleration, α_c, which is directly associated with foundation capacity, M_{ult}, and, hence, decreases with reducing foundation size. The effectiveness of rocking isolation in terms of inertial loading is summarized in Fig. 17. Evidently, the two underdesigned foundations (medium and small) drastically reduce the maximum acceleration, α_{max}, transmitted to the deck for all studied seismic excitations.

2. Despite having quite different FS values, the medium and small foundations sustain practically the same moment loading and consequently permit similar levels of inertial loading to be transmitted onto the superstructure. This similarity in their capacity can be attributed to two observations: (1) lateral load capacity is principally controlled by the slenderness ratio, h/L, and is insensitive to changes in the foundation out-of-plane dimension; and (2) during cyclic loading, an overstrength mechanism was observed to take place and affect mainly the capacity of small foundations.
3. FS_V affects the development and accumulation of permanent displacements. Fig. 18 illustrates the accumulation of settlement during the complete sequence of seismic excitations, revealing that, as expected, the decrease in FS_V leads to increased settlement.
4. At least for the case of the symmetric seismic motions investigated herein, the increase of settlement appears to be the only significant argument against the rocking isolation concept (i.e., underdesigning the foundation for the sake of structural safety). Yet, the problem reduces to defining the acceptable

J. Geotech. Geoenviron. Eng. 2012.138:1369-1386.

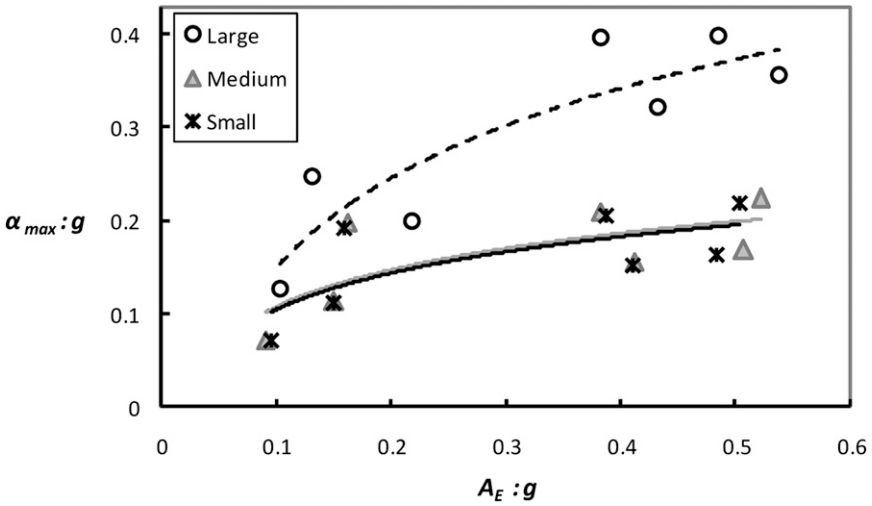

Fig. 17. Rocking isolation effectiveness for the three pier-foundation systems: maximum deck acceleration α_{max} versus the acceleration amplitude A_E of the base excitation; note that the indicated continuous lines are the result of curve fitting to the corresponding data points

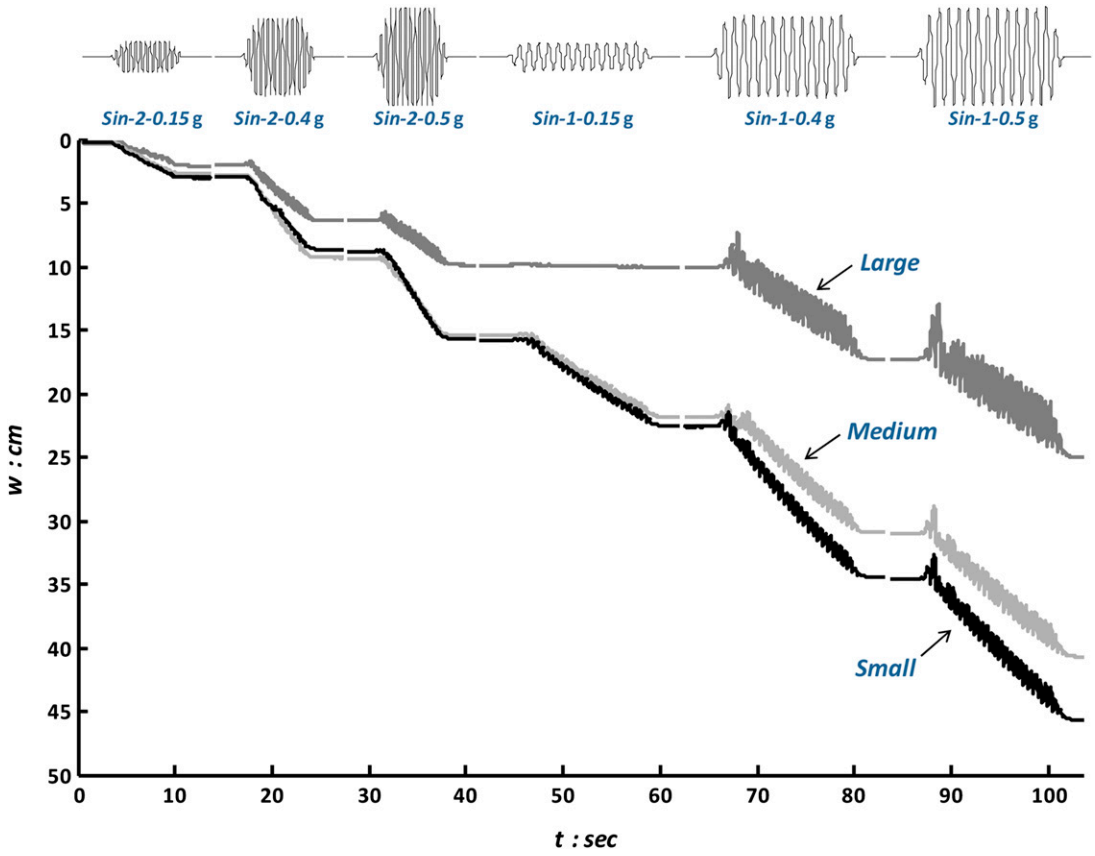

Fig. 18. Evolution of foundation settlement with the applied sequence of sinusoidal seismic shaking

displacements of the superstructure in relationship with performance requirements.

5. Owing to the inherent symmetry of the sine-type seismic excitations, the three foundations did not suffer considerable permanent rotation. However, real earthquake excitations include sometimes deleterious asymmetric pulses, which may cause significant permanent foundation rotation. Such effects merit a separate study.

Limitations

The herein presented study has been based on a set of reduced scale $1g$ physical tests. Inherently prone to scale effects when applied to geotechnical problems, reduced scale modeling may yet yield valid results, if such effects are taken into account in the design of the experiments and in the interpretation of results. Scale effects were sufficiently mitigated through appropriate modeling of the foundation systems

J. Geotech. Geoenviron. Eng. 2012.138:1369-1386.

aiming to achieve similarity between model and prototype in terms of the load-capacity analogy in both the vertical and lateral (in-plane) directions. Yet, although considered adequate for the specific problem studied herein (rocking in one direction), the reader should bear in mind that the general validity of the presented foundation modeling concept suffers from the misreproduction of foundation shape effects.

Acknowledgments

The research was funded by the European Research Council (ERC) program *"IDEAS, Support for Frontier Research − Advanced Grant"*, under contract number ERC−2008−AdG 228254−DARE.

Notation

The following symbols are used in this paper:

A_E = maximum acceleration at bedrock;
B = out-of-plane foundation breadth;
C_u = uniformity coefficient;
D_r = relative density;
D_{10} = maximum grain size of the finest 10%;
D_{50} = mean grain size;
D_{60} = maximum grain size of the finest 60%;
$e_{\max}$ = void ratio at the loosest state;
$e_{\min}$ = void ratio at the densest state;
FS_E = factor of safety in combined *N-Q-M* loading;
FS_V = factor of safety in pure vertical loading;
f_E = excitation frequency;
G_s = specific weight of solids;
h = height of the oscillator;
h_f = foundation height;
h_p = distance from the top of the foundation to the center of mass;
L = in-plane foundation breadth;
M = moment load;
M_{ult} = ultimate moment load;
m = mass;
N = vertical load;
N_{ult} = ultimate vertical load;
n = modeling scale;
Q = shear load;
R = overstrength ratio;
S_a = spectral acceleration;
T = period;
u_H = foundation horizontal translation (swaying component);
w = foundation settlement;
α = acceleration at the center of mass;
α_c = critical acceleration ($a_c = M_{ult}/mgh$);
$\alpha_{\max}$ = maximum acceleration at the center of mass;
δ = deck total drift;
θ = foundation rotation;
φ = soil friction angle; and
φ' = effective soil friction angle.

References

Allotey, N., and El Naggar, M. H. (2003). "Analytical moment−Rotation curves for rigid foundations based on a Winkler model." *Soil. Dyn. Earthquake Eng.*, 23(5), 367−381.

Allotey, N., and El Naggar, M. H. (2008). "An investigation into the Winkler modeling of the cyclic response of rigid footings." *Soil. Dyn. Earthquake Eng.*, 28(1), 44−57.

Anastasopoulos, I., Gazetas, G., Loli, M., Apostolou, M., and Gerolymos, N. (2010a). "Soil failure can be used for seismic protection of structures." *Bull. Earthquake Eng.*, 8(2), 309−326.

Anastasopoulos, I., Gelagoti, F., Kourkoullis, R., and Gazetas, G. (2011). "Simplified constitutive model for simulation of cyclic response of shallow foundations: Validation against laboratory tests." *J. Geotech. Geoenviron. Eng.*, 137(12), 1154−1168.

Anastasopoulos, I., Georgarakos, P., Georgiannou, V., Drosos, V., and Kourkoulis, R. (2010b). "Seismic performance of bar-mat reinforced-soil retaining wall: Shaking table testing versus numerical analysis with modified kinematic hardening constitutive model." *Soil. Dyn. Earthquake Eng.*, 30(10), 1089−1105.

Beck, J. L., and Skinner, R. I. (1973). "The seismic response of a reinforced concrete bridge pier designed to step." *Earthquake Eng. Struct. Dyn.*, 2(4), 343−358.

Bolton, M. D. (1986). "The strength and dilatancy of sands." *Geotechnique*, 36(1), 65−78.

Bransby, M. F., and Randolph, M. F. (1998). "Combined loading of skirted foundations." *Geotechnique*, 48(5), 637−655.

Butterfield, R., and Gottardi, G. (1994). "A complete three dimensional failure envelope for shallow footings on sand." *Geotechnique*, 44(1), 181−184.

Chatzigogos, C. T., Pecker, A., and Salencon, J. (2009). "Macroelement modelling of shallow foundations." *Soil. Dyn. Earthquake Eng.*, 29(5), 765−781.

Chen, Y. H., Liao, W. H., Lee, C. L., and Wang, Y. P. (2006). "Seismic isolation of viaduct piers by means of a rocking mechanism." *Earthquake Eng. Struct. Dyn.*, 35(6), 713−736.

Chopra, A., and Yim, S. (1985). "Simplified earthquake analysis of structures with foundation uplift." *J. Struct. Eng.*, 111(4), 906−930.

Cremer, C., Pecker, A., and Davenne, L. (2001). "Cyclic macro-element for soil structure interaction—Material and geometrical nonlinearities." *Numer. Met. Geomech.*, 25(13), 1257−1284.

Cremer, C., Pecker, A., and Davenne, L. (2002). "Modelling of non linear dynamic behaviour of a shallow strip foundation with macro-element." *J. Earthquake Eng.*, 6(2), 175−212.

Faccioli, E., Paolucci, R., and Vivero, G. (2001), "Investigation of seismic soil-footing interaction by large scale cyclic tests and analytical models." *Proc., 4th Int. Conf. Recent Adv. Geotech. Earthquake Eng. Soil Dyn.*, Missouri Univ. of Science and Technology, Rolla, MO, 26−31.

Figini, R. (2010). "Nonlinear dynamic soil-structure interaction: Application to the seismic analysis and design of structures on shallow foundations." Ph.D. dissertation, Polytechnico di Milano, Milan, Italy.

Gajan, S., and Kutter, B. L. (2008). "Capacity, settlement, and energy dissipation of shallow footings subjected to rocking." *J. Geotech. Geoenviron. Eng.*, 134(8), 1129−1141.

Gajan, S., and Kutter, B. L. (2009). "Contact interface model for shallow foundations subjected to combined loading." *J. Geotech. Geoenviron. Eng.*, 135(3), 407−419.

Gajan, S., Kutter, B. L., Phalen, J. D., Hutchinson, T. C., and Martin, G. (2005). "Centrifuge modeling of load-deformation behavior of rocking shallow foundations." *Soil. Dyn. Earthquake Eng.*, 25(7−10), 773−783.

Gazetas, G., Anastasopoulos, I., and Apostolou, M. (2007). "Shallow and deep foundations under fault rupture or strong seismic shaking." Chapter 9, *Earthquake geotechnical engineering*, K. Pitilakis, ed., Springer, Dordrecht, Netherlands, 185−215.

Georgiadis, M., and Butterfield, R. (1988). "Displacements of footings on sand under eccentric and inclined loads." *Can. Geotech. J.*, 25(2), 199−212.

Gottardi, G., and Butterfield, R. (1993). "On the bearing capacity of surface footings on sand under general planar loads." *Soil Found.*, 33(3), 68−79.

Gottardi, G., Houlsby, G. T., and Butterfield, R. (1999). "Plastic response of circular footings on sand under general planar loading." *Geotechnique*, 49(4), 453−469.

Gourvenec, S. (2007). "Shape effects on the capacity of rectangular footings under general loading." *Geotechnique*, 57(8), 637−646.

Harden, C., Hutchinson, T., and Moore, M. (2006). "Investigation into the effects of foundation uplift on simplified seismic design procedures." *Earthquake Spectra*, 22(3), 663−692.

J. Geotech. Geoenviron. Eng. 2012.138:1369-1386.

Housner, G. W. (1963). "The behavior of inverted pendulum structures during earthquakes." *Bull. Seismol. Soc. Am.*, 53(2), 404−417.
Huckelbridge, A. A. and Clough, R. W. (1978). "Seismic response of uplifting building frames." *J. Struct. Eng.,*104(8), 1211−1229.
Huckelbridge, A. A., and Ferencz, R. M. (1981). "Overturning effects on stiffened building frames." *Earthquake Eng. Struct. Dyn.*, 9(1), 69−83.
Martin, G. R., and Lam, I. P. (2000). "Earthquake resistant design of foundations: retrofit of existing foundations." *Proc., GeoEng 2000 Conf.* (CD-ROM), Melbourne, Australia, 19−24.
Meek, J. W. (1978). "Dynamic response of tipping core buildings." *Earthquake Eng. Struct. Dyn.*, 6(5), 437−454.
Mergos, P. E., and Kawashima, K. (2005). "Rocking isolation of a typical bridge pier on spread foundation." *J. Earthquake Eng.*, 9(2), 395−414.
Meyerhof, G. G. (1951). "The ultimate bearing capacity of foundations." *Geotechnique*, 2(4), 301−332.
Meyerhof, G. G. (1953). "The bearing capacity of foundations under eccentric and inclined loads." *Proc., 3rd Int. Conf. Soil Mech. Found. Eng.*, Zurich, Switzerland, Vol. 1, 440−445.
Moncarz, P. D., and Krawinkler, H. (1981), "Theory and application of experimental model analysis in earthquake engineering." *Rep. No. 50*, Dept. of Civil Engineering and Environmental Engineering, Stanford Univ., Stanford, CA.
Montrasio, L. and Nova, R. (1997). "Settlements of shallow foundations on sand: Geometric effects." *Geotechnique*, 47(1), 49−60.
Muir Wood, D. (2004). *Geotechnical modelling*, Spon Press, London.
Negro, P., Paolucci, R., Pedrett, S., and Faccioli, E. (2000). "Large−scale soil−structure interaction experiments on sand under cyclic loading." *Proc., 12th World Conf. Earthquake Eng.* (CD-ROM), Auckland, New Zealand, 1191.
Nova, R., and Montrasio, L. (1991). "Settlements of shallow foundations on sand." *Geotechnique*, 41(2), 243−256.
Panagiotidou, A. I. (2010). "2D and 3D inelastic seismic response analysis of foundation with uplifting and P−Δ effects." Diploma thesis, National Technical Univ., Athens, Greece.
Paolucci, R., Shirato, M., and Yilmaz, M. T. (2008). "Seismic behavior of shallow foundations: Shaking table experiments vs numerical modeling." *Earthquake Eng. Struct. Dyn.*, 37(4), 577−595.
Pecker, A. (2005), "Design and construction of the foundations of the Rion Antirion Bridge." *Proc., 1st Greece−Japan Workshop on Seismic Design, Observation, Retrofit of Foundations*, National Technical Univ. of Athens, Athens, Greece, 119−130.
Pecker, A., and Pender, M. (2000). "Earthquake resistant design of foundations: new construction." *Proc., GeoEng 2000 Conf.* (CD-ROM), Melbourne, Australia, 313−334.
Priestley, M. J. N., Evison, R. J., and Carr, A. J. (1978). "Seismic response of structures free to rock on their foundations." *Bull. N. Z. Soc. Earthquake Eng.*, 11(3), 141−150.
Priestley, M. J. N., Seible, F., and Calvi, G. M. (1996). *Seismic design and retrofit of bridges*, Wiley, New York.
Psycharis, I. N., and Jennings, P. C. (1983). "Rocking of slender rigid bodies allowed to uplift." *Earthquake Eng. Struct. Dyn.*, 11(1), 57−76.
Raychowdhury, P., and Hutchinson, T. C. (2009). "Performance evaluation of a nonlinear Winkler-based shallow foundation model using centrifuge tests results." *Earthquake Eng. Struct. Dyn.*, 38(5), 679−698.
Sakellaraki, D., and Kawashima, K. (2006), "Effectiveness of seismic rocking isolation of bridges based on shake table tests." *Proc., 1st Euro. Conf. Earthquake Eng. Seismol.* (CD-ROM), Geneva, Switzerland, 1−10.
Taiebat, H. A., and Carter, J. P. (2000). "Numerical studies of the bearing capacity of shallow foundations on cohesive soil subjected to combined loading." *Geotechnique*, 50(4), 409−418.
Ticof, J. (1977). "Surface footings on sand under general planar loads." Ph.D. thesis, Southampton Univ., Southampton, U.K.
Ukritchon, B., Whittle, A. J., and Sloan, S. W. (1998). "Undrained limit analysis for combined loading of strip footings on clay." *J. Geotech. Geoenviron. Eng.*, 124(3), 265−279.
Vesic, A. S. (1973). "Analysis of ultimate loads of shallow foundations." *J. Soil Mech. Found. Div.*, 99(1), 45−73.

J. Geotech. Geoenviron. Eng. 2012.138:1369-1386.